

Materials and Innovations for Large Blade Structures: Research Opportunities in Wind Energy Technology

Thomas D. Ashwill[§]

Sandia National Laboratories, Albuquerque, New Mexico 87185*

The significant growth in wind turbine installations in the past few years has fueled new scenarios that envision even larger expansion of U.S. wind electricity generation from the current 1.5% to 20% by 2030. Such goals are achievable and would reduce carbon dioxide emissions and energy dependency on foreign sources. In conjunction with such growth are the enhanced opportunities for manufacturers, developers, and researchers to participate in this renewable energy sector. Ongoing research activities at the National Renewable Energy Laboratory and Sandia National Laboratories will continue to contribute to these opportunities. This paper focuses on describing the current research efforts at Sandia's wind energy department, which are primarily aimed at developing large rotors that are lighter, more reliable and produce more energy.

I. Introduction

Wind energy as a utility power source continued to expand dramatically in 2008. Figure 1 [1] shows the yearly and cumulative installed capacity in the United States from 1995 to 2007, with 2008's entry as an estimate. The actual installed capacity in the U.S. has exceeded most, if not all, expectations and predictions over the past several years. The 2008 number actually came in at 8.5 GW, as reported by AWEA (www.awea.org), well ahead of an estimated 6.5 GW. It is expected that the 2009 number will be down due to financial market pressures, but new orders are expected to pick up again in 2010. Installed wind energy capacity worldwide has also grown exponentially over the past few years, and BTM predictions [1] are that this growth will continue for many years (Fig. 2).

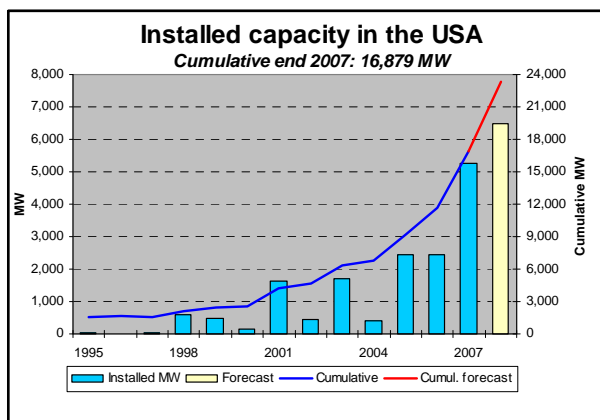


Figure 1. U.S. Installed, Utility-Grade Wind Energy Capacity by BTM [1]

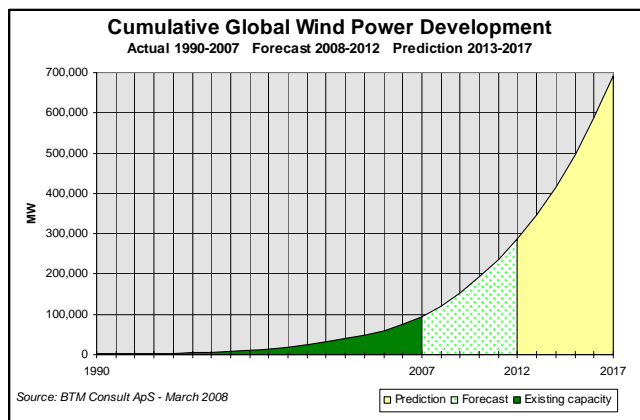


Figure 2. Cumulative Global Wind Power Development: Historical and Predicted by BTM [1]

[§] Technical Staff, Wind Energy Dept., MS1124, Senior Member AIAA

* Sandia is a multiprogram laboratory operated by Sandia Corporation, a Lockheed Martin Company for the United States Department of Energy's National Nuclear Security Administration under contract DE-AC04-94AL85000.

The inflation-adjusted cost of energy (COE) for wind power has fallen dramatically as well (at least up until the last two years when turbine demand and extra-high commodity price rises took effect). The cost of wind energy has dropped from over 80 cents/kWh in 1980 to as low as 5 cents/kWh today [2]. A major part of this decrease has to do with the inherent efficiencies associated with larger turbines. Their physical size has increased from an average of 100 kW in 1985 to over 2.0 MW today (2009) with commercial turbines being built that are up to 6 MW in size, and even larger ones on the drawing board. Figure 3 shows a graphic of turbine rotor growth over the past 24 years.

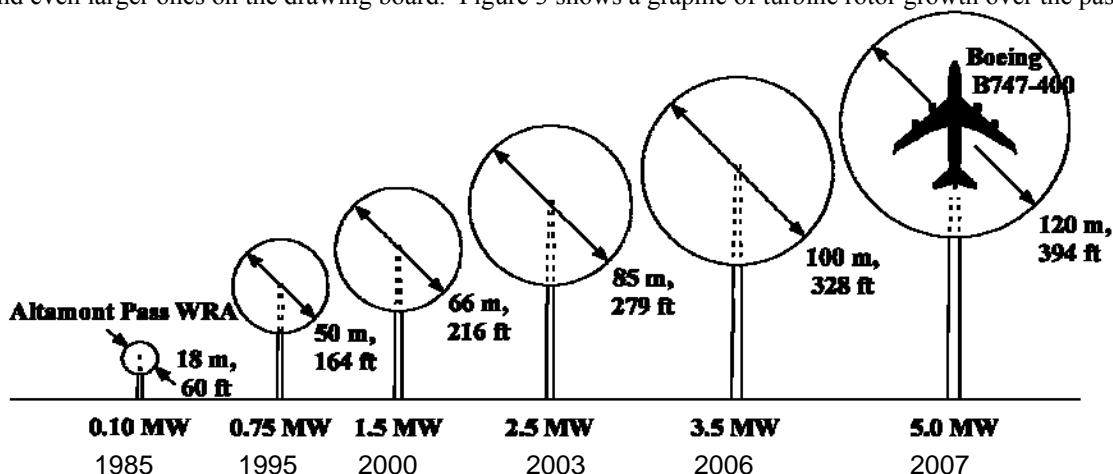


Figure 3. Turbine Rotor Growth Since 1985

This paper focuses on describing the ongoing research activities at Sandia's wind energy department, which are primarily aimed at developing large rotors that are lighter, more reliable and produce more energy. The following sections will describe results from our prime areas of work which are materials, manufacturing, structural codes, structurally efficient airfoils, active and passive load control, sensors, and prototype development with testing.

II. Wind Turbine Technology and General Research

Turbines, to the surprise of many, are complex (and very large) machines. A 2.3 MW turbine (See Fig. 4), the average sized utility grade turbine today, rises some 80 m to the hub and has a rotor diameter of approximately 82 m. It may weigh on the order of 300,000 kg including blades, nacelle and tower. To achieve maximum performance, complicated control systems must manage the turbine in highly turbulent winds with its multiple degrees of freedom, including nacelle yaw, blade pitch and variable rotor rpm. The drive train and power electronics must convert variable frequency AC to DC to constant frequency AC to match the line frequency and voltage. The turbine has to withstand hurricane level winds and operate to a design life of 20 years.

However, the industry seems to have a handle on the complexity and has matured to the degree that wind turbines can now be certified by agencies such as Germanischer Lloyd (GL) and DNV to standards like the International Electrotechnical Commission (IEC) that prescribe design conditions reflecting the knowledge and experience of many industry experts that sit on IEC Annex Committees.

A number of aeroelastic codes with full simulation capabilities are available for use by the wind industry. The National Renewable Energy Laboratory's (NREL's) FAST code (for Fatigue, Aerodynamics, Structures, and Turbulence) is an aeroelastic simulator that predicts both the extreme and fatigue loads of 2-bladed and 3-bladed Horizontal Axis Wind Turbines (HAWT's). ADAMS (Automated Dynamic Analysis of Mechanical Systems), developed by MSC Software, is a general-purpose, multi-body dynamics code with unlimited degrees of freedom that can model almost any kind of HAWT. Both codes require NREL's AeroDyn subroutine library to model aerodynamics. European codes include Garrad Hassan's GH Bladed, a widely accepted European code, and GL's DHAT, both of which are similar to FAST.

Codes such as NuMAD (Sandia), PreCOMP (NREL), and 3DBeam (Stanford) can assist with detailed composite blade design and analysis.



Figure 4. Siemens 2.3 MW Turbines

Research to make turbines more efficient and durable with relatively lower costs continues not only at national laboratories but at large turbine companies themselves, many of whom have significant research budgets. The U.S. DOE Wind and Hydropower Technology Program [2] has a goal of improving the efficiency and lowering the costs of conventional wind turbine technologies. This is performed by conducting a program of research and development that leads to improvements in large and small wind turbine industries. The Wind Program conducts activities to support these goals with a coordinated partnership between DOE, NREL, Sandia National Labs, other national laboratories, universities, industry and other independent organizations, such as the National Wind Coordinating Committee. As mentioned previously, COE has dropped significantly; however, a further goal is to reduce costs to the point of being competitive with all sources of utility grade power *without* the U.S. production tax credit (PTC). Research and development efforts will also play an important role in the “20% wind by 2030 scenario” described in Ref. 3, where the technical feasibility of using wind to generate 20% of the nation’s electricity by 2030 is explored.

III. Overview of Research at Sandia National Laboratories

A. Innovations

Sandia is creating concepts that will enable the utilization of longer blades that weigh less, are more efficient structurally and aerodynamically, and impart reduced loads to the system [4]. One of the prime goals for blade developments is to keep blade weight growth under control. Gravity scales as the cube of the blade length and as turbines continue to grow, gravity loads become a constraining design factor. This weight growth can be slowed down by becoming more efficient in design methodology. Figure 5 shows blade weight growth trends as a function of rotor radius from commercial data and DOE-sponsored WindPACT preliminary designs [5]. Here we can observe trend lines of older commercial designs, newer commercial designs, and designs that have come out of the WindPACT studies [6] that incorporate new concepts. It is possible to lower the growth rate from an exponent of 3.0 to one of 2.5 by incorporating design innovations.

B. Specific Concepts

The following are examples of concepts being developed:

- 1) More efficient blade structures (thick airfoils, designs that fully integrate structure and aerodynamics, and slenderized blade geometries).
- 2) Adaptive structures for load control (passive and active).
- 3) Materials and manufacturing improvements, involving
 - a) new materials for wind turbine blades such as carbon, carbon-hybrid, S-glass and new material forms
 - b) design details to minimize stress concentrations in ply drop regions
 - c) less expensive, embedded blade attachment devices.

C. Structural Codes

To support blade research activities, analytical capabilities are continually improved. Two examples are the composite design tool, NuMAD, and a flutter prediction capability.

NuMAD is a user-friendly, windows based (GUI) pre-processor and post-processor for the ANSYS commercial finite element engine [7]. It is designed to enable users to quickly and easily create a three-dimensional model of a turbine blade and perform structural and modal analyses. The user inputs blade geometry, such as chord and twist distribution, and lay-up details. An airfoil and material database are readily available to assist in model creation. While users need no previous knowledge of the ANSYS analysis package, experience with finite element methods is required to use NuMAD effectively. Figure 6 is a screen shot of a blade model being created in NuMAD before meshing.

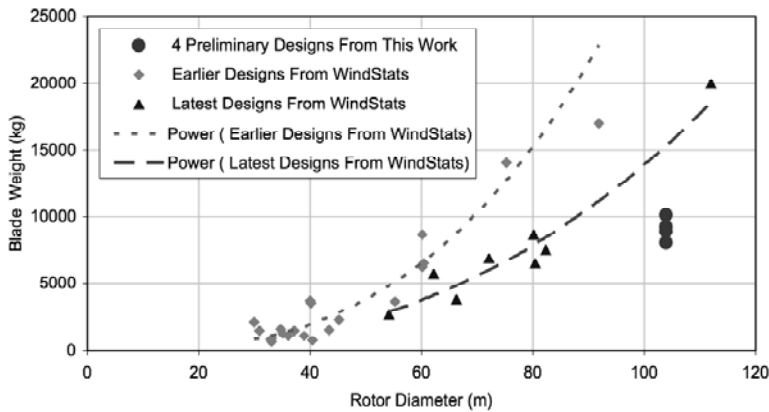


Figure 5. Blade Weight vs. Rotor

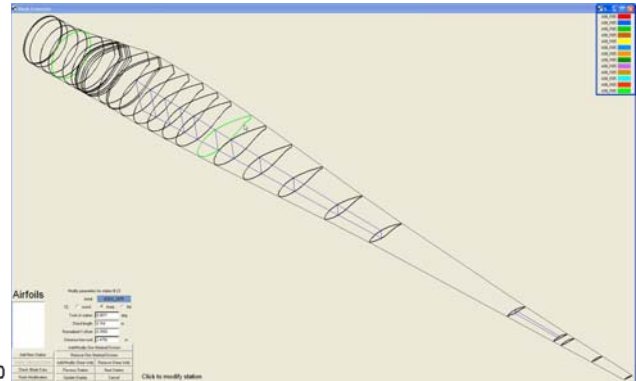


Figure 6. NuMAD Model Creation

Classical aeroelastic flutter has generally not been a driving issue in utility scale wind turbine design, but there is concern that it is becoming more of a design constraint because larger turbines are fitted with relatively softer blades. Innovative blade designs that use aeroelastic tailoring, wherein the blade twists as it bends under the action of aerodynamic loads to shed load resulting from wind turbulence, increase the blades tendency to flutter. Years ago Sandia developed a methodology to estimate flutter speed and aerodynamic damping for Vertical Axis Wind Turbines (VAWT's) [8], and more recently Lobitz applied this technique to flutter stability predictions for HAWT's. [9]. Commercial finite element software, MSC NASTRAN (www.mscsoftware.com), is used for this aeroelastic stability estimation procedure. NASTRAN can accommodate non-symmetric, complex-valued matrices as are required in this effort and provides a number of complex eigenvalue solvers for the stability analysis. The blades are modeled with NASTRAN beam (CBEAM) elements, which do not have a provision for the coupling between bending and twisting that is required for aeroelastic tailoring. Consequently, additional terms are added to the stiffness matrix in the manner described in [10,11] to affect this coupling. Additional terms are also added to the various matrices to provide for rotating coordinate system effects (Coriolis and centrifugal softening terms) using the procedure outlined in [11]. The outputs from this calculation are mode shapes and associated damping. Flutter instability is predicted to occur at the rpm when damping of the lowest frequency blade mode becomes negative.

IV. Composite Material Testing

Sandia's materials testing program currently consists primarily of testing and analyzing coupon fatigue tests for a variety of composite lay-ups. The following sections provide selections of relevant test results emanating from recent material-related projects.

A. Recent Coupon Fatigue Tests at MSU

For many years, Sandia has had an ongoing effort to characterize composite materials for wind turbine use. Much of the related fatigue testing of composite materials is performed by Montana State University (MSU), which first published the DOE/MSU Composite Material Fatigue database in 1997 [12,13]. This document, which is updated yearly, contains the results of static and fatigue coupon testing of commercially-available composite materials. Recent testing shows the fatigue resistance for several wind turbine blade materials as detailed in the next sections.

1) Effects of Fiber Type. The effects of fiber type on tension and compression fatigue resistance are shown in Figure 7, where the stress and strain based fatigue resistance in tension ($R = 0.1$) and compression ($R = 10$) are compared [14,15].

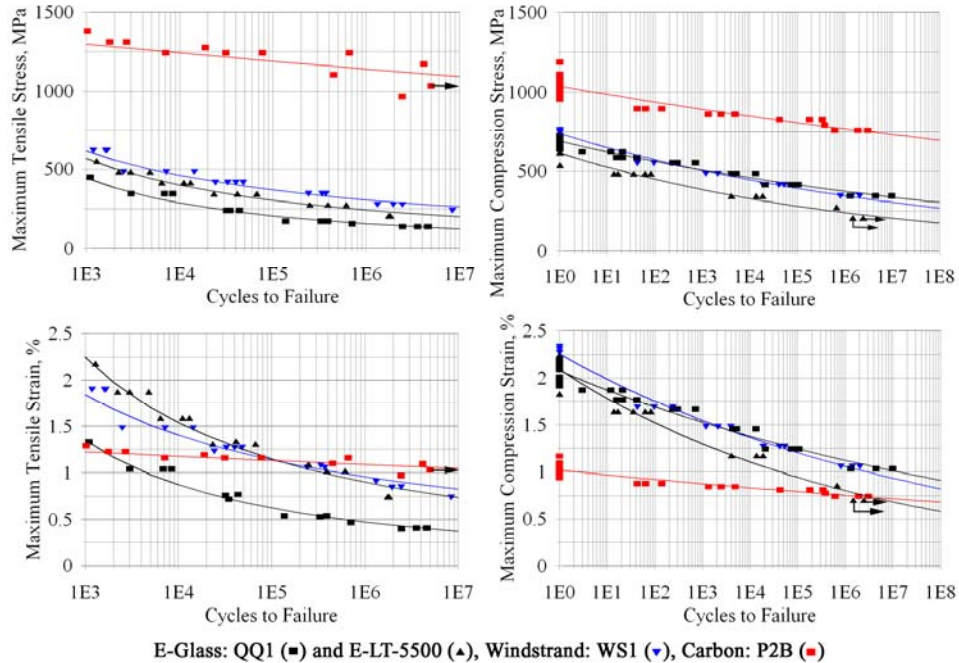


Figure 7. Fatigue Comparison of Multidirectional Laminates. Based on E-glass (QQ1 and E-LT-5500), WindStrand™ (WS1) and carbon (P2B) fibers at similar fiber contents, in terms of stress (top) and strain (bottom), epoxy resins, $R = 0.1$ (left side) and $R = 10$ (right side).

The four laminates, representing three main fiber types all with epoxy resins, are

- E-glass (or Advantex™), QQ1
- E-LT- 5500-EP
- WindStrand™, WS1
- Carbon hybrid (Grafil 34-600, 48k tow), P2B.

The laminates have differing contents of 0° plies relative to $\pm 45^\circ$ plies, slightly different fiber contents, and different processing. Notable differences in fatigue performance are that the carbon hybrid is superior in terms of stress and shows a much less steep fatigue curve compared to the glass fiber materials at $R = 0.1$ (tension). The compression fatigue curve for carbon is also less steep. Of the glass laminates, QQ1 is notably less tensile fatigue resistant and E-LT-5500-EP is less compression fatigue resistant. WindStrand™ is generally similar to the best of the E-glass laminates in each case, but slightly stronger in terms of stress, in tension. The aligned strand structure of the WindStrand™ WS1 laminates may be advantageous compared with stitched fabrics used for QQ1 and E-LT-5500 [16].

2) Carbon Reinforcement. Carbon fiber reinforced laminates for wind blades are most limited by compressive strength and ultimate strain [17, 18]. Additionally, the presence of even minor amounts of fiber misalignment has been shown to reduce static and fatigue properties significantly [19]. Maximum compressive properties are obtained with laminates which have the straightest fiber alignment, generally unidirectional prepreg 0° plies; poorest properties have been found with woven fabrics, particularly with large tow. Figure 8 compares the compressive static and fatigue properties for three carbon fiber materials: P2B, relatively thick (0.3 mm) prepreg with unidirectional carbon fiber 0° plies; MMWK C/G-EP, infused triaxial fabric with $+45^\circ$ and -45° E-glass plies sandwiching 0° carbon strands; and CGD4, VARTM processed 0° stitched carbon fabric with E-glass $\pm 45^\circ$ plies. The P2B laminate gives properties typical of other large tow prepreps [16,17]. The CGD4 laminate is among the best stitched or bonded carbon fabrics tested [17], but not as good as the prepreg, apparently due to slight misalignment in the fabric strands. The MMWK-C/G-EP laminate properties were at least equivalent to various prepreps tested in this program, with very straight strands held in place by the glass 45° 's. This fabric contains about 25% off-axis material by volume which reduces the strength and modulus values relative to 100%-unidirectional carbon laminates [16].

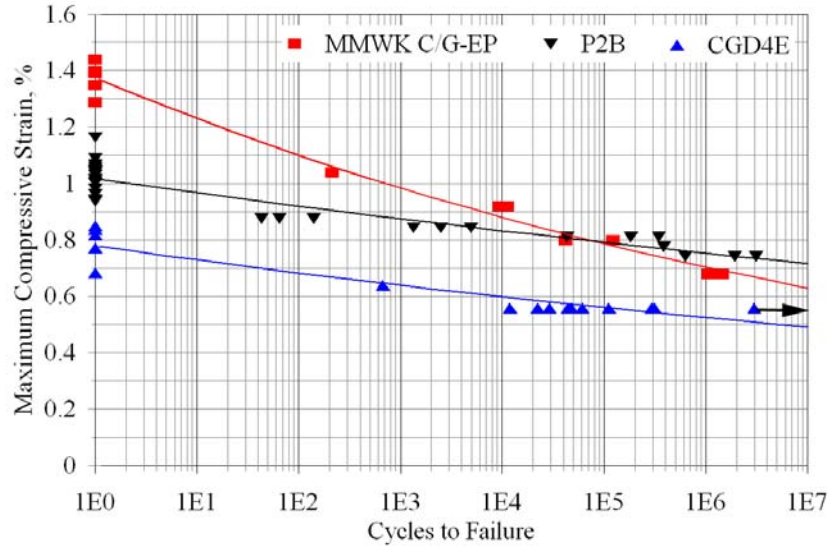


Figure 8. Comparison of Compressive Fatigue Resistance of Hybrid Laminates with Carbon 0° plies and E-glass ±45° Plies. Materials: P2B (prepreg); MMWK C/G-EP (infused stitched hybrid triaxial fabric); and CGD4E (VARTM stitched fabrics) at R = 10.

3) Summary of Issues and Conclusions. Conditions (major issues) have been identified which can produce severe fatigue damage or failure in good quality coupons at maximum absolute strains in the range of 0.2 to 0.4%:

- Glass fiber laminates with less fatigue resistant fabric architectures at higher fiber contents, loaded in tensile fatigue with R-values in the -0.5 to 0.1 range.
- Delamination at ply drops and ply joints, for plies greater than 1.0 mm thickness for glass fibers, or 0.6 mm for carbon fibers (most R-values).
- Matrix cracking in off-axis plies, for R-values with a significant tensile component (glass and carbon fiber laminates, various resins).
- Carbon fiber laminate compressive strength and its sensitivity to fabric or other fiber waviness.
- Delamination and adhesive failure in complex details under both static and fatigue loading.
- Hot/wet conditions, which can exacerbate these issues (with the exception of the first).

Major conclusions are (see Refs. 15,16,20,21 for more detail):

- The relatively new WindStrand™ based laminates, in addition to moderately higher modulus, show very good fatigue resistance under both tension and compression loading, compared to E-glass.
- Carbon, either prepreg or the infused triax hybrid fabric, is very fatigue resistant under all loading conditions; other infused fabrics have shown reduced compression resistance [17].
- Delamination resistance under pure and mixed modes is strongly matrix dependent, with epoxies generally providing the most resistance [17]. Ply drop delamination at high fatigue cycles occurs at low strains regardless of R-value, position through the thickness or overall laminate thickness. The thickness of material dropped at a single position is an important geometric parameter; improvements have been demonstrated [16,18,21] for treatments of the ply drop edge, including chamfering and pinking.

B. BSDS-Phase II Project

Under the SNL-sponsored, GEC-directed Blade System Design Studies (BSDS) contract, alternative composite materials, manufacturing processes, and structural designs were evaluated for potential benefits for MW-scale blades [22,23]. The BSDS-Phase I project partly consisted of trade-off studies to identify alternative materials and manufacturing approaches to support the development of longer and lighter utility-grade blades. The primary objectives of BSDS-Part II were to perform coupon and sub-structure testing for the evaluation of material and process combinations with promise for application to MW-scale blades. The Phase II final report was recently published. [16].

Testing of composite articles was performed at three laboratories: Integrated Technologies (Intec) in Everett, Washington; Montana State University (MSU) in Bozeman; and Wichita State University (WSU). Efforts were made to ensure that the program is complementary with the DOE/MSU Database testing at Montana State University [12].

Composite materials evaluated include carbon fiber in both pre-impregnated and vacuum-assisted resin transfer molding (VARTM) forms. Thin-coupon static testing incorporated a wide range of parameters, such as variation in manufacturer, fiber tow size, fabric architecture, and resin type. A smaller set of these materials and process types was evaluated in thin-coupon fatigue testing, and in ply-drop and ply-transition panels. The majority of materials used epoxy resin, however vinyl ester (VE) resin was also used for selected cases. Testing of unidirectional fiberglass was added late in the project to provide an updated baseline against which to evaluate the carbon material performance.

Numerous unidirectional carbon fabrics were considered for evaluation with VARTM infusion. All but one fabric style considered suffered either from poor infusibility or waviness of fibers combined with poor compaction. The exception was a triaxial carbon-fiberglass fabric produced by SAERTEX. This fabric became the primary choice for infused articles throughout the test program. The generally positive results obtained in this program for the SAERTEX material have led to its use in innovative prototype blades of 9-m and 30-m length.

As noted above, obtaining good structural performance with a VARTM process presents significant manufacturing challenges. Figure 9 shows how stitching can adversely affect the straightness of carbon fibers in a unidirectional fabric.

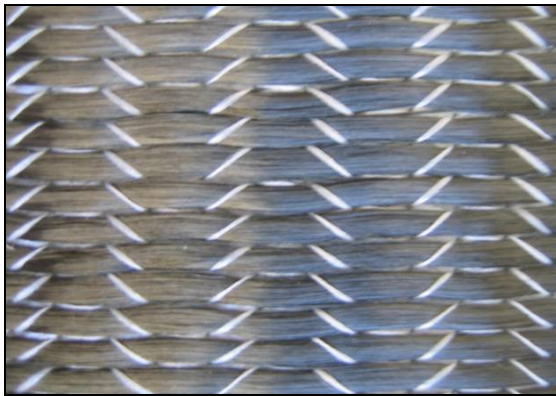


Figure 9. Stitched Fabric with Manufacturing-Induced Waviness

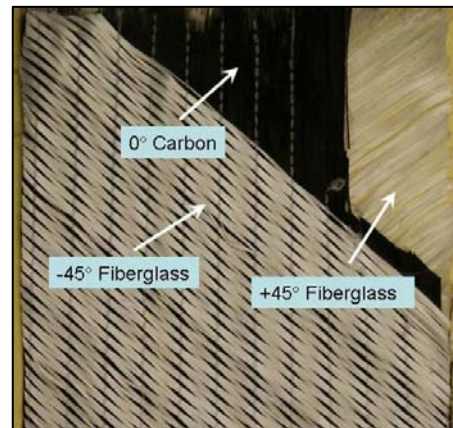


Figure 10. SAERTEX Triaxial Carbon-Fiberglass Fabric

Figure 10 shows the most favorable fabric identified, a multi-layer, multi-axial warp-knit (MMWK) style produced by SAERTEX. GEC worked with the vendor and TPI Composites to develop this architecture. The fabric is a triaxial construction $[-45^{\circ}_{\text{Glass}}/0^{\circ}_{\text{Carbon}}/+45^{\circ}_{\text{Glass}}]$ with areal weights of 150/670/150 grams/m². The net fiber content is 75% carbon and 25% fiberglass by volume. Distinct features of this architecture and SAERTEX stitching style include those listed below:

- the outer layers are fiberglass, providing some protection of carbon fibers;
- the stitching pattern is such that it squeezes the glass strands, but runs parallel with and between strands of carbon fibers;
- the resulting fabric has good infusibility without introducing waviness in the carbon fibers; and
- the triaxial construction provides good stability for material handling.

1) Ply Drop Panels. To study the effects on ply delaminations due to ply drops in the material, two styles of panels with ply drops were fabricated: drops with standard straight edges and drops with pinked edges as illustrated in Figure 11. The motivation for fabricating and testing the panels with the pinked ply drops was to reduce the stress concentration at the ply drop edge. Both the straight and pinked configurations were fabricated in prepreg and infused articles.

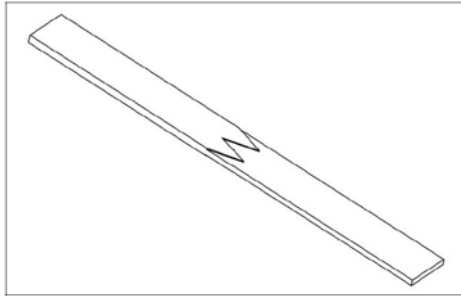


Figure 11. Pinked Ply Drops

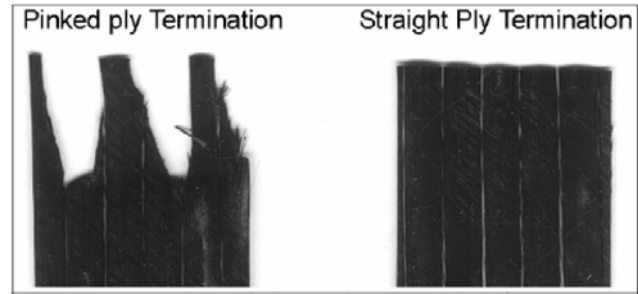


Figure 12. Face View of Ply Terminations.

Carbon fiber is difficult to cut and Figure 12 shows that the accuracy of the pinking in the SAERTEX fabric is far from ideal. By contrast, the tacky nature of prepreg materials makes precise cutting much easier.

Asymmetries in the ply drop coupons due to manufacturing issues created challenges for obtaining reliable results in compression testing. Therefore, the majority of fatigue testing for the ply drop specimens was performed in tension ($R=0.1$). Ply drops were tested in both straight and pinked edge geometries.

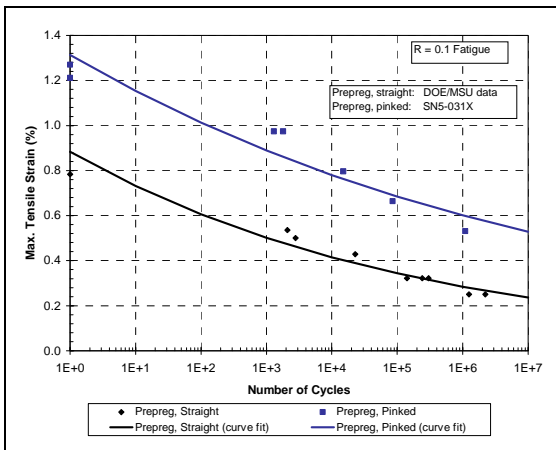


Figure 13: Tensile Data for Prepreg Ply Drop Specimens

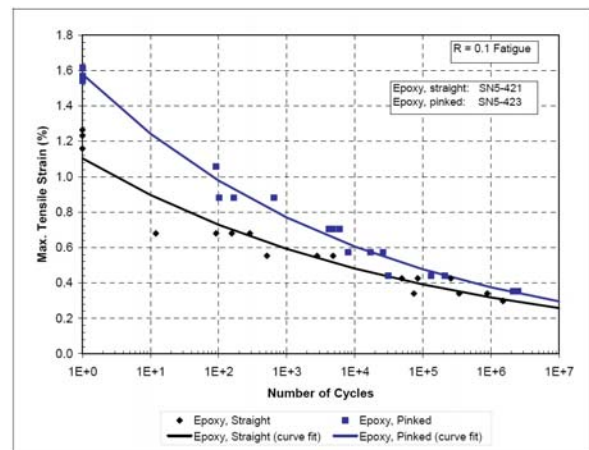


Figure 14: Tensile Data for Infused Epoxy Straight and Pinked Ply Drops.

Figure 13 shows results for ply drop panels manufactured at Montana State University (MSU) using Grafil/Newport prepreg material. The data represent the number of cycles required to develop a delamination of 6.35 mm (0.25 inch). As indicated in Figure 13, for the straight ply drop (control) the strain level for 10^6 cycle delamination is below 0.3%. The fatigue performance for the pinked coupon is greatly improved, with 10^6 strain increased to above 0.5%.

Figure 14 shows results for infused ply drop panels manufactured at TPI using SAERTEX carbon-fiberglass triax fabric with epoxy, in both straight and pinked configurations. For the straight-edge configuration, the 10^6 strain is about 0.3%. The improvement due to pinking is less than was seen for the prepreg materials, with 10^6 strain values increase to about 0.4%. The trends for both epoxy and VE resins are quite similar [16].

For all fabric and resin styles, a ply drop with a straight edge resulted in lower fatigue performance than the same fabric and resin with a pinked ply drop. For prepreg laminate, the introduction of a pinked-ply drop edge nearly doubled the strain level for delamination at 10^6 cycles. With the infused fabrics, the pinked edge showed far less benefit, with a strain improvement at 10^6 cycles of about 25%. The relatively low fatigue performance for the infused ply drops with pinking may be partly due to the geometry of the ply drops and panels.

2) Infused Fiberglass Fatigue Results. Figure 15 shows fatigue data ($R = 0.1$ and 10) for the E-LT-5500 fiberglass fabric, infused with both epoxy and VE resins. Strain values in these figures were calculated by GEC based on the MSU-measured stress levels combined with the average modulus measured by Intec in static testing.

The tension ϵ -N curve of Figure 15 shows several trends. For both the epoxy and VE resins, the intersection of the curves at zero cycles is substantially higher than the measured single-cycle strain. At higher cycles, the VE tension fatigue strength falls consistently below that of the epoxy.

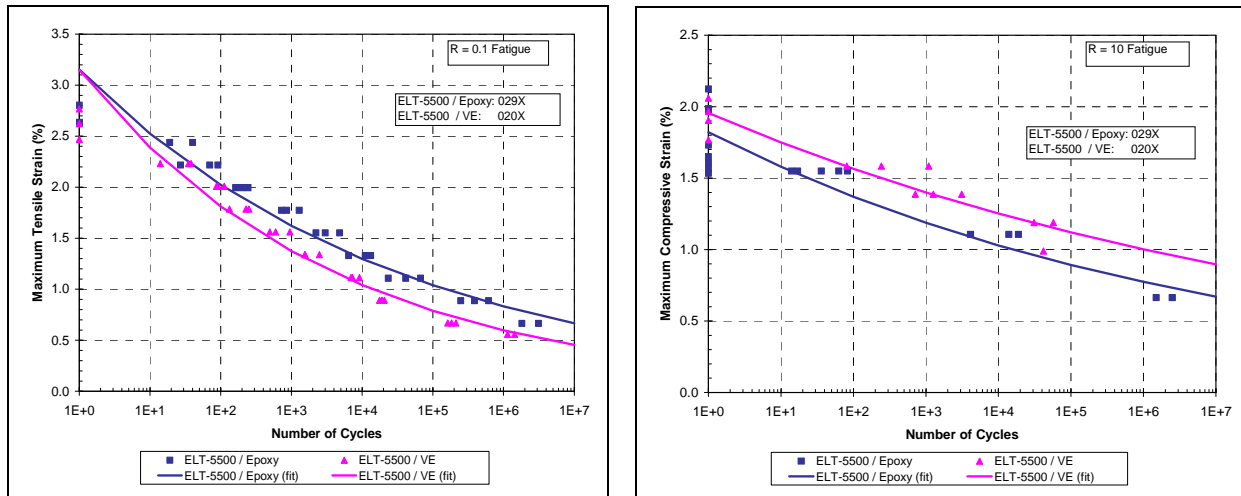


Figure 15. R = 0.1 (left) & 10 (right) Fatigue Data for Thin-coupon Infused Fiberglass.

Significantly different trends are seen in the compressive strain fatigue data. Most notable is that the VE data fall consistently above that of the epoxy. The curves are also flatter than those seen for the R = 0.1 data (i.e. they have a higher fatigue exponent).

V. Manufacturing

Our manufacturing research has historically been aligned with characterizing details of the process and its effects on material properties. For example, as documented in Ref. 24, Cairns and Skramstad compared material properties of laminates and substructures fabricated by hand lay-up and resin transfer molding techniques. Reference 25 documents the simulation and testing of a resin infusion process for large composite structures. Figure 16 shows the test fixture fabricated at MSU [25] that characterizes the porosity and fluid flow properties (permeability) of different forms of composite materials. A process flow model was validated in conjunction with this work.

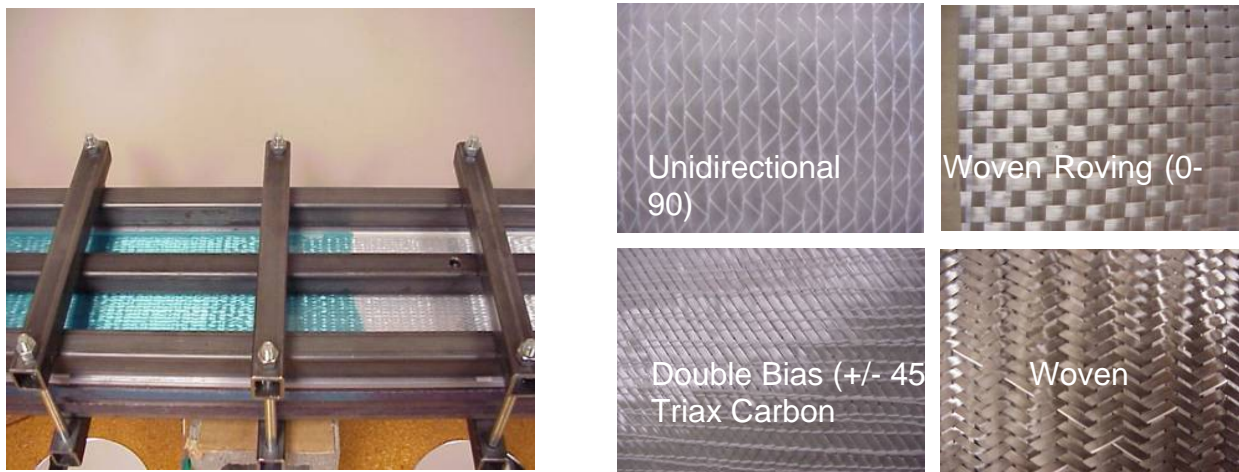


Figure 16. Permeability Testing of Glass and Carbon Fabrics

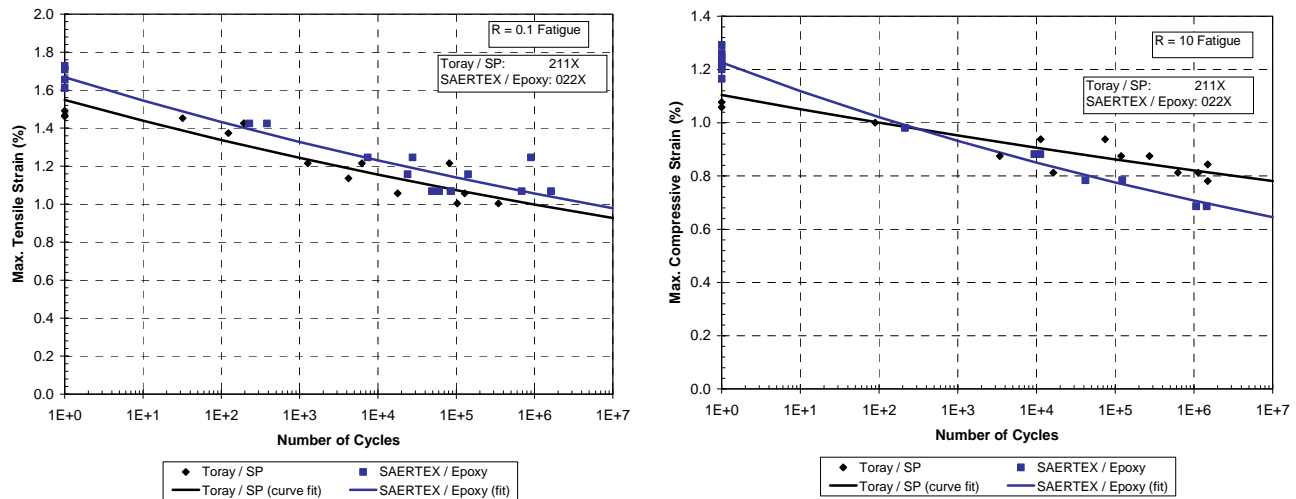


Figure 17. Effects of Different Manufacturing Processes: Pre-preg and Infused Carbon Epoxy @ R = 0.1 & 10

The effects of two different fabrication processes on fatigue life are shown in Fig. 17, which compares fatigue data for prepreg and infused (epoxy) carbon panels [16]. The infused panels use the SAERTEX carbon-fiberglass triaxial fabric with a substantial amount of integral $\pm 45^\circ$ fiberglass fibers, whereas the prepreg panels are primarily unidirectional carbon tape, with a small amount of $\pm 45^\circ$ glass in the facings. Consequently, the modulus of the infused panels is by design lower than the prepreg materials. In terms of evaluating the performance of the carbon fibers in the laminate, a comparison of strain levels provides a more valid basis than does the stress.

The R = 0.1 data for Toray prepreg and epoxy-infused triax panels indicates that the overall performance for these materials is quite similar. Strain values for the infused article are modestly higher than those for the prepreg over the entire range of cycles. A somewhat different trend exists for the R = 10 fatigue. At the single-cycle end of the ϵ -N curve, the infused triax panel strains are about 10% higher than the prepreg, but at 10^6 cycles, the triax strains fall below the prepreg by 20%. The R = 10 slope is steeper for the infused material. The prepreg ϵ -N curve has a slope parameter of $m \approx 46$, whereas the triax has an $m \approx 25$. Comparisons for R = -1 (fully reversed fatigue) loading show very close agreement between the infused material and the Toray prepreg [16].

VI. Airfoils for Structural Efficiency & Noise Measurements

A. Flatback Airfoil Development

A Sandia WindPACT Blade System Design Study (BSDS) produced several innovations for large blades [6, 26]. As part of this study, the TPI-Dynamic Design-UC Davis team came up with the idea of using very thick airfoils with significantly expanded trailing edge thicknesses at the root to enhance structural capability. Led by Case van Dam of UC Davis, the team performed a systematic investigation on the use of a series of inboard airfoils whose thickness and trailing-edge flat could be adjusted independently to give a constant thickness for the spar cap and trailing-edge spline. This series of airfoils was developed from high-lift inboard NREL airfoils and the LS-1 series airfoils. Representative inboard section shapes are shown in Fig. 18 and are labeled as “flatback” airfoils to denote the lift-enhancing trailing edge flat. These airfoils are different from blunt trailing edge profiles in that they retain trailing edge camber [26]. Aerodynamic performance characteristics of the airfoils were predicted using computational techniques that properly simulate blunt trailing edge flows. The thick flatback airfoils are shown to have excellent lift characteristics that are much less sensitive to surface soiling than conventional sharp-trailing-edge airfoils of equal thickness. Figure 19 provides lift and drag curves for the flatback compared to a sharp, trailing edge baseline for both clean and soiled conditions. These airfoils have potential for decreasing COE because the thicker sections allow for a lighter blade (higher moment of inertia) and the increase lift characteristics could allow for enhanced performance. However, the drag also increases, and it is expected that trailing edge treatment, such as splitter plates may be required to reduce the increased drag (see next section). A 9-m prototype research blade, BSDS Phase II, was fabricated that include flatbacks on the inner 50%. This blade has been tested in the laboratory for structural performance (see Section VIII) and will be flown on the test turbines at the USDA site in Bushland, Texas later this year.

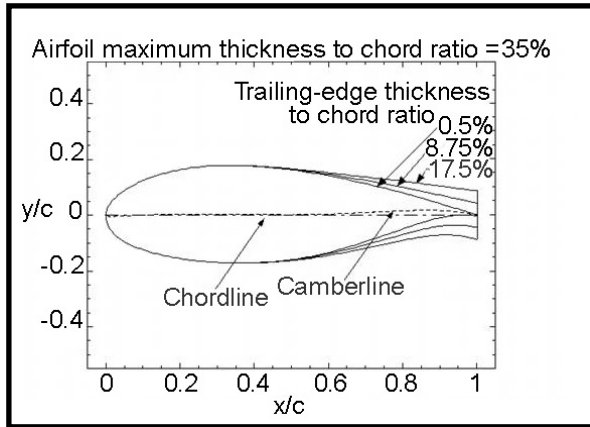


Figure 18. Flatback Airfoils

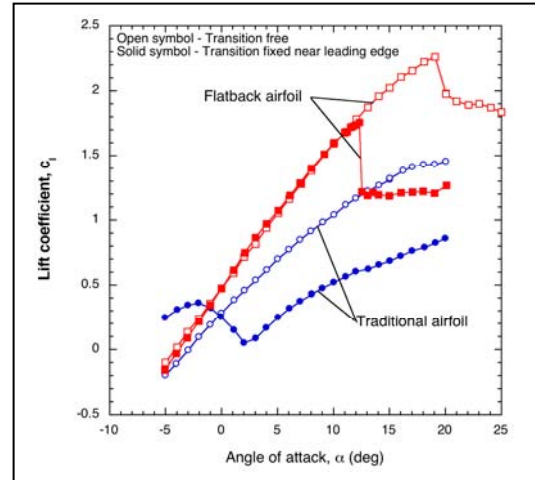


Figure 19. C_l for Flatback & Traditional Airfoils – Clean & Soiled

B. Aerodynamic and Aeroacoustic Testing of Flatback Airfoils

The technical risks associated with the use of flatback airfoils for the inboard region of wind turbine blades are increased aerodynamic drag and aerodynamic noise. Both penalties are the result of the blunt trailing edge shape and wake produced by this shape. Figure 20 is a picture of a CFD simulation of flow over a flatback airfoil (notice the vortex shedding). The effect of this drag penalty on rotor thrust and torque coefficient for typical inboard twist angles is not severe and can be offset by the additional lift that a flatback airfoil generates [27]. Consideration of drag reducing devices such as splitter plates or trailing edge serrations is desirable to further boost performance.

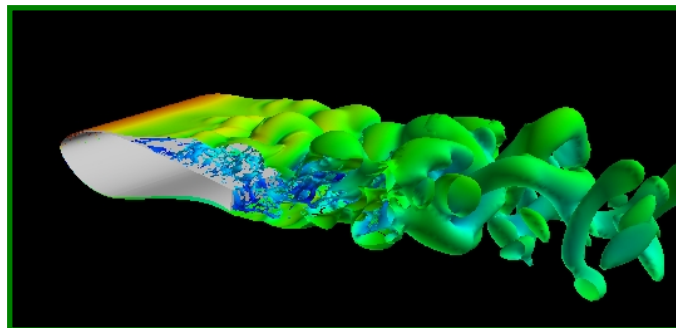


Figure 20. Flatback CFD Simulation

As stated in Ref. 28, “The increased noise from the flatback is due primarily to the vortex shedding phenomenon associated with bluffbody wakes.....Since outboard flow velocities are much higher than those encountered inboard, the overall aerodynamic noise levels of a rotor incorporating inboard flatback shapes will likely continue to be dominated by outboard trailing edge noise. However, two aspects of the flatback noise source may be cause for concern. First, the vortex-shedding noise from flatbacks is likely to be contained in a relatively low-frequency band (50-200 Hz). Some community noise regulations have separate low-frequency noise standards apart from consideration of A-weighted sound, which emphasize higher frequencies to which the human ear is more sensitive. Second, the source of the flatback noise is likely to be tonal in nature. Pure tones are perceived as more annoying than broadband noise, often resulting in special treatment of tones in noise standards.”

Previous work on flatback airfoils includes wind tunnel testing at moderate Reynolds numbers [29] and computational modeling of flatback airfoils and their effect on rotor performance [27, 30]. Reference 28 reports on more recent work on flatbacks that 1) measured aerodynamic performance at higher Reynolds numbers (3 million) representative of that encountered by utility scale turbines, 2) quantified the drag penalty and aeroacoustic noise, 3) assessed the effect of a simple splitter plate attachment on flatback drag and noise, and 4) validated computational models of flatback aerodynamics and aeroacoustics against experimental data.

To this end, a wind tunnel experiment was performed to measure the aerodynamic and aeroacoustic characteristics of the TU-Delft DU97-W-300 airfoils and a flatback version of that airfoil, the DU97-flatback (see Fig. 21). The DU97-flatback was created by adding thickness to the aft half of the airfoil, giving a blunt trailing edge with a width of 10% chord.

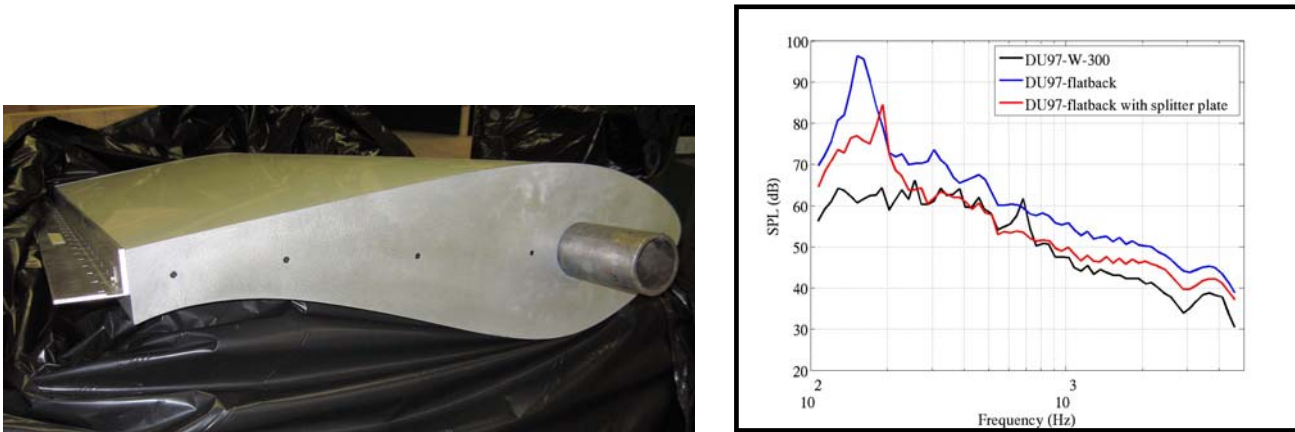


Figure 21. Flatback Noise Measurements with & without Splitter Plates

Aerodynamic measurements are reported in Ref. 28 and indicate that drag penalties can be reduced by up to 50% using a simple splitter plate (Fig. 21). The aeroacoustic testing showed that flatbacks can create a significant increase in broadband noise. The addition of splitter plate reduces this noise significantly at most frequencies and lower angles of attack (Fig. 21). These noise measurements are also used as a basis for validating aeroacoustic models. The increase in the lift curve slope and maximum lift coefficient reported at lower Re numbers [6,26] is also seen at the higher Re number of 3,000,000.

VII. Passive Load Control

Previous work has shown the potential for modifying blade design to incorporate bend-twist coupling in ways to passively reduce loads at high winds [31-36]. Incorporating bend-twist coupling into the blade allows the designer to grow the turbine rotor in diameter using longer blades while maintaining the same fatigue loads and thus capturing more energy at a small capital cost increase.

For passive load control using bend-twist coupling, blades can be designed in a least two different ways. One is to sweep the blade along the span to create a moment that induces twist [37]. A second method is to align the primary load-carrying spanwise fibers in an off-axis manner by about 20 degrees, so as the blade bends, it twists more than normal allowing loads to be relieved. The idea was to effectively allow more coupling between the flap and twist motions of the blade. Necessary goals are to maintain flapwise strength and maximum tip deflection. Studies have shown that this “bend-twist” coupling is maximized with the use of very stiff fibers, such as carbon [38]. A series of concepts studies were performed for Sandia in 2002 that developed detailed methods for actually implementing such ideas into a blade [36]. One of the prototype blades fabricated (see next section) is termed the TX-100 and incorporates carbon in the skin at 20 degrees off-axis. This blade was tested and resulted in bend-twist coupling with its enhanced twisting. In the Knight & Carver (K&C) project a 27-m swept blade was designed, fabricated and tested. This successful project, further discussed later in this paper, increased the blade length by 10% and increased energy capture by 5-8%.

VIII. Active Load Control

Load control can be established through individual or collective pitch of the blades [39]. An alternative methodology that has some advantages over pitch control is the use of active aerodynamic devices. Active aerodynamic load control devices have the potential to reduce fatigue loads on turbine blades to levels below that of current collective blade pitch control technology. Distributed control devices can respond to local loads whereas pitch control moves the entire blade based on an integrated load measurement, like torque for example. Active aerodynamic control devices that will be most effective in controlling loads are found to be those that alter the effective camber of the blade. Thin airfoil theory shows that these devices are most effective when installed at the blade trailing edge. Research work of Sandia and its university contractors initially

focused on small devices known as microtabs. More recently we have begun to study morphing trailing edge devices (morphing flaps).

A. Microtabs

Microtabs are particularly attractive because of their simple shape and quick response. Simulations have shown they exert significant control authority, but many challenges must be solved before the economic feasibility of such a device can be demonstrated.

Tabs are typically deployed approximately perpendicular to the airfoil surface to a height that is about equal to the thickness of the boundary layer (1-2% chord) [40]. The deployment effectively alters the camber as shown in Figure 22, which pictures streamlines around an airfoil with microtabs from computation simulations. Deployment on the pressure side of the airfoil increases lift and on the suction side deployment mitigates lift. Research efforts to study microtabs have been ongoing at UC Davis since the late 1990's [41]. Effects of tab height, location and spacing were all investigated and show that a tab height of 1% chord, located at 95% of chord towards the trailing edge, on the lower surface provides the best compromise for lift and drag [42]. 2-D computational efforts have been validated in the wind tunnel for the S809 airfoil with microtabs [43]. Full aeroelastic simulation of the NREL CART turbine with microtabs and pitch control demonstrated that it is possible to significantly reduce tip deflection and root bending moments [44]. Further wind tunnel tests are underway to investigate microtab operation in conjunction with a controller.

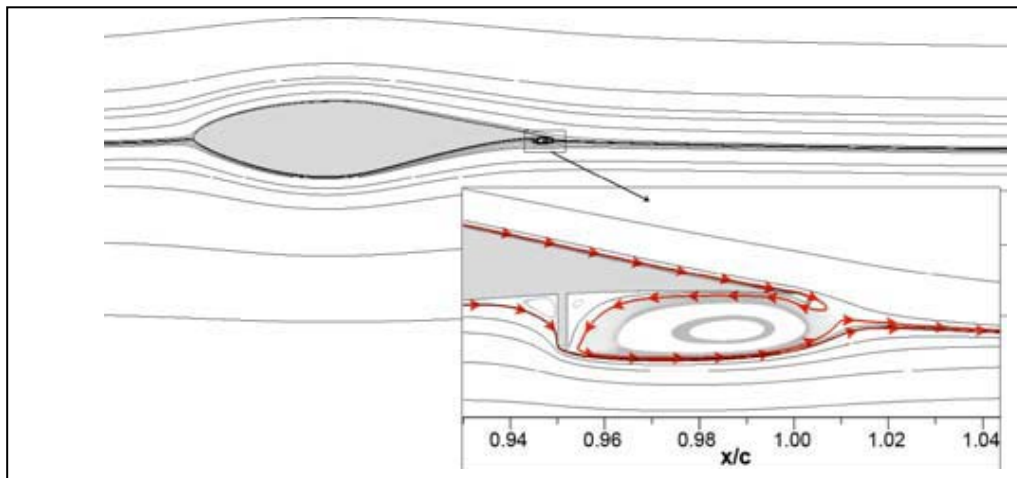


Figure 22. Instantaneous Streamlines of an S809 Airfoil with 1.1% Chord Pressure Surface Tab Located at 95% Chord

B. Morphing Trailing Edges

It has been shown by researchers at Delft Technical University (TU Delft) [45] and Risø National Laboratory/Danish Technical University [46] that active aerodynamic load control potentially can decrease blade flap fatigue loads on a turbine rotor by significant amounts. Lackner and van Kuik recently reported on a study of the load reduction capabilities of load control using conventional flaps on a 5MW turbine [47]. In “Active Load Control Techniques for Wind Turbines”[40], Johnson, et. al. provides a comprehensive list of devices that could be used for active flow control. Among the promising technologies are flap-type devices, including conventional flaps and morphing trailing edges [48].

FlexSys Inc, of Ann Arbor, Michigan has produced morphing trailing edges for aircraft wings [49] that use distributed-compliance mechanisms that depend on elastic deformation of their elements to transmit motion and/or forces. A morphing trailing edge is a structure that contours to pre-determined aerodynamic shapes while creating a smooth and continuous surface and supporting aerodynamic loads. Minimizing actuator forces and maintaining adequate lifetimes of operation are design drivers. These structures can be quickly and smoothly deflected toward either the pressure or suction surface of the wing to form an effective flap, while avoiding the surface discontinuities and air gaps common to conventional flap systems. The compliant structure is optimized to minimize actuator effort and maximize the airfoil surface stiffness to air loading. The morphed flap has a lift characteristic comparable to that of a conventional flap, but with a significant reduction in drag increment during extreme flap deflections. Figure 23 illustrates morphed trailing edges deployed at 20° on an NREL S825 wind-turbine airfoil. The smooth surfaces of the morphed trailing edges are far less likely to cause flow separation than are the surface discontinuities of conventional flaps.

Sandia is working with FlexSys [50] to further develop the application of this morphing trailing edge technology to wind turbine blades and has performed extensive simulations, using the WindPACT 1.5 MW turbine and two different control algorithms. Results estimate the increased energy capture and benefits of integrating the FlexSys technology into the tip region of the turbine blades. This work has shown that, within the limitations of the FAST/AeroDyn simulation (having no torsional degrees of freedom), adding active aerodynamic load control devices to a 1.5 MW turbine, has a significant impact on the fatigue damage accumulations at several critical turbine locations. This may result in 10% or more additional energy capture after increasing the rotor to a size that would experience the same fatigue damage as the smaller baseline. Full sets of simulations will be required to determine if additional fatigue damage occurs to the turbine drive train and tower.

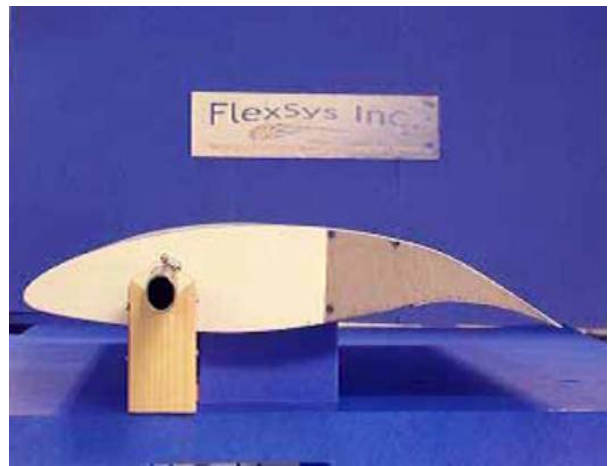


Figure 23. FlexSys Morphing Trailing Edge Demonstration

IX. Sensors

Sandia has an ongoing program to identify and test sensors for wind turbine applications. For blade applications, there is a need for real-time sensing to maximize structural and aerodynamic efficiency, support advanced control strategies, and detect damage for structural health monitoring (SHM). Reference 51 provides results of the testing of a variety of low-cost sensors after embedment in composite laminates. Two sensor application projects that are nearly complete are the Sensor Blade I and SHM implementation into a prototype.

A. Sensor Blade I

A sensor blade (9-m CX-100), termed the SBlade I (Fig. 24), has been fabricated to incorporate a suite of sensors that could provide relevant information during turbine operation. These include embedded and surface mounted FBG (fiber Bragg grating), metal foil strain gauges, RTD temperature, streaming video for blade shape measurements, and accelerometers for blade shape, loads and SHM. Flight testing is underway, and static laboratory tests are complete. Flight data will be analyzed to determine the feasibility of the various sensors vs. their placement, location and usefulness. One technique developed by Purdue University will use accelerometer data (inertial measurements) from an operating turbine and estimate quasi-static distributed loading and deflection of the rotor blade [52]. This technique will be validated against flight data as it becomes available. Sensor Blade II is in planning stages and will test the feasibility of a variety of wind in-flow sensors for real-time sensing.



Figure 24. Installation of Sensors During SBlade I Fabrication

B. Structural Health Monitoring

Structural health monitoring devices were attached to the TX-100 prototype blade and monitored during its fatigue test [53]. The blade eventually failed due to buckling at the maximum chord location. The main sensor/sensor systems installed are: Physical Acoustics Corporation (PAC) acoustic emission (AE) NDT system, NASA wave propagation-based SHM, accelerometers (Purdue SHM system), Virginia Tech impedance-based SHM system, photoelastic panels (load/strain path detection) and strain gauges. The PAC AE NDT system did detect significant AE events early in the test, but had some uncertainty associated with locating the events because of diversity of materials in a composite blade, which result in acoustic energy attenuation and velocity anisotropy. The impedance and wave propagation-based SHM techniques were probably too far away from the failure location to yield useful results; further analysis and testing is underway. The ability to measure tip deflection using an accelerometer was promising. Overall, this test shows the difficulty in using SHM in a large structure; the challenge is to use an array of sensors wide enough to monitor the entire structure but yet can detect damage that often initially occurs at small scale, nonspecific locations. Continued efforts will determine the most appropriate SHM techniques, ways to process the resulting information to affect turbine operation decisions, and cost-effectiveness.

X. Prototype Blades and Testing

A. 9 Meter Prototypes

In 2002 SNL initiated a research program [4] to demonstrate the use of carbon fiber in subscale blades and investigate innovative concepts through the WindPACT Blade System Design Studies (BSDS) via design studies and Phase II prototype fabrication [54,6]. From these projects, three 9-m designs were created with assistance from Global Energy Systems Consulting (GEC), Dynamic Design Engineering, and MDZ Consulting; and seven blades from each design were manufactured by TPI Composites. All blades were designed for a 100 kW stall controlled turbine. The first blade set was called CX-100 (Carbon Experimental), and contained a full-length carbon spar cap, a relatively new concept at the time. The geometry of the CX-100 was based on the design of the ERS-100 [55] blade at outboard span stations, and the Northern Power Systems NW-100 blade in the root area.

The second blade design, the TX-100 (Twist-Bend Experimental), had the same geometry as the CX-100, but was designed to have passive load reduction by orienting unidirectional carbon 20° off of the pitch axis in the skins from approximately 25% span outward. As discussed earlier, studies had showed the potential of such a method of passive aeroelastic load alleviation through material induced twist-bend coupling, with 20° being determined as the optimum angle. The TX-100 also contained a fiberglass spar cap which terminated at the mid-span of the blade.

The third blade design was termed the BSDS (Blade System Design Studies), the name of the research solicitation under which it was created. The BSDS has a length of 8.325 m rather than the 9.000 m length of the CX-100 and TX-100. This blade design included features as a thin-walled, large-diameter root; flatback airfoils; integrated root studs; and a full-length, constant-thickness, carbon spar cap.

A drawing of these blades is shown in Figure 25 with the carbon areas shown in blue. Note the carbon spar caps of the CX-100 and the BSDS blades, and the carbon outboard skins of the TX-100. The unidirectional fiberglass spar cap of the TX-100 is shown in red and extends only to the mid-span of the blade. It was determined that the large amount of carbon contained in the skin was adequate to carry loads outboard in this design, making a full length spar cap unnecessary. The narrow, constant thickness spar cap of the BSDS blade indicates the inherent structural stiffness of this design. In addition, the BSDS design (Fig. 26) features a more gradual transition between the root and max-chord areas as compared to the CX and TX platform.

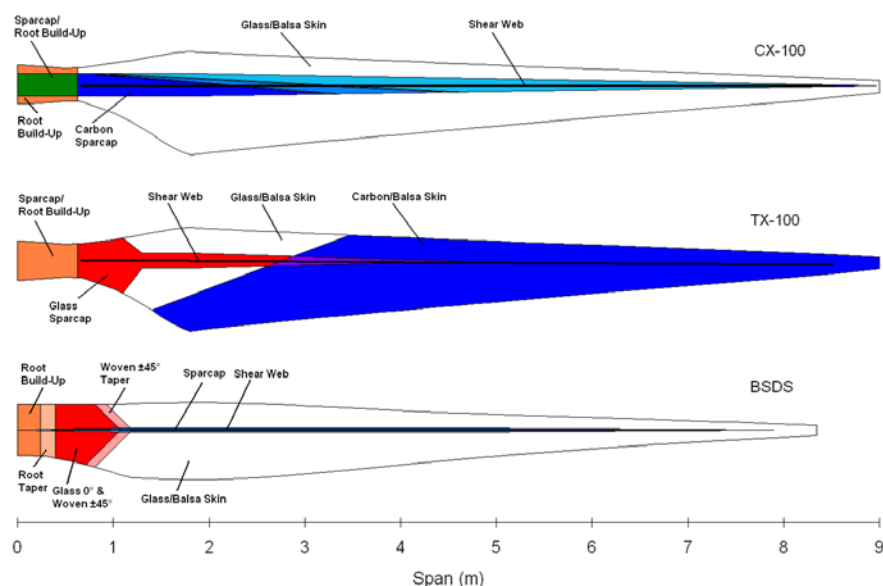


Figure 25. 9 m Blade Plan Form and Major Material Regions

A suite of laboratory and field tests are verifying the extent to which the manufactured blades meet their design goals [56]. To date, specimens from each design have undergone successful modal, static and fatigue testing.

1) Static Testing. One blade from each design set was statically tested to failure at the National Wind Technology Center (NWTC) due to a flapwise bending load case that approximates the extreme loading events for the wind class to which each blade was designed [57]. All blades were loaded by use of a three-point whiffle tree (Fig. 27) and saddle connected to an overhead bridge crane. For the TX-100 blade test, a rope and pulley arrangement was attached to the saddles in an attempt to allow twisting without altering the loading point. The blades were loaded and unloaded in increasing 25%



Figure 26. Root End of BSDS Prototype Blade Showing Flatbacks and Embedded Anchor Rods

increments up to the 100% test load. Also, an array of sensors was used in the tests to monitor strain, deflection, load, and acoustic emissions.

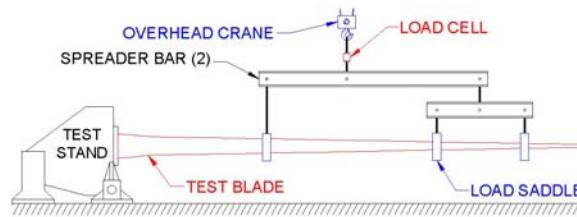


Figure 27. NREL’s Whiffle Tree Loading Arrangement

Acoustic emissions sensed by microphones placed on the blade surface can be used to indicate the location of damage that occurs in the blade during testing. An example the use of this technology is shown in Figure 28 for the CX-100 static test where measured acoustic events are overlaid on an outline of the blade. Each event is color coded with a relative energy range, which represents the integral of the voltage vs. time curve. Although not the true energy, these voltage vs. time results are useful for comparative purposes. During the CX-100 test, several high-energy events were located between 1.20 m and 1.30 m along the spar cap. The CX-100 blade was observed during failure to experience a catastrophic buckling of the low-pressure skin near the 1.2-m station. A post mortem inspection of the blade in this region did indeed show a large crack in the bond joint between the low pressure skin and the shear web.

A summary of results of the static tests of all three blade designs is contained in Table 1. The relatively high strength of the BSDS blade is evident, with the measured carbon strains approaching values seen in coupon testing of pre-preg specimens. This high strength combined with the significantly lower weight points to the structural advantages of this design in comparison to the CX-100 and TX-100, which were both significantly better performers than the baseline ERS-100.

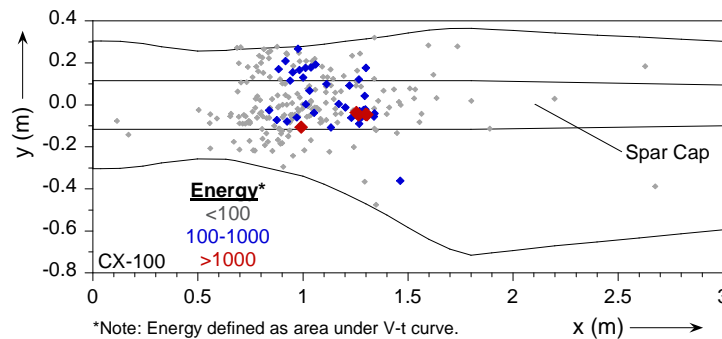


Figure 28: Acoustic Event Locations and Energies for CX-100 Static Test.

Table 1: Summary of Results of 9-m Blade Tests.

Property	CX-100	TX-100	BSDS
Weight (lb)	383	361	289
% of Design Load at Failure	115%	197%	310%
Root Failure Moment (kN-m)	128.6	121.4	203.9
Max. Carbon Tensile Strain at Failure (%)	0.31%	0.59%	0.81%
Max. Carbon Compressive Strain at Failure (%)	0.30%	0.73%	0.87%
Maximum Tip Displacement (m)	1.05	1.80	2.79

All three test blades survived factored design test loading. The CX-100 blade displayed exceptional stiffness, deflecting only 1.05 m at a root moment of 128.6 kN-m. The blade failed due to panel buckling near max-chord which was likely initiated by a separation between the shear web and the low-pressure skin in that region. The TX-100 blade successfully demonstrated twist-bend coupling caused by 20°-off-axis carbon in the outboard skins as seen in Figure 29, which compares measured and predicted twist distribution along the blade [58]. The TX-100 blade failed at a slightly lower load than the CX-

100 blade, but in a similar location. The BSDS blade displayed exceptional strength in comparison to the CX-100 and TX-100 designs, surviving to almost three times the target test load. The flatback airfoil feature performed well and did not display non-linear behavior until well after the target test load was reached. In addition, the root mounting studs of the BSDS blade were observed to have good static loading properties. Finally, the acoustic emission monitoring system detected not only the locations where damage was occurring, but also incipient global blade failure.

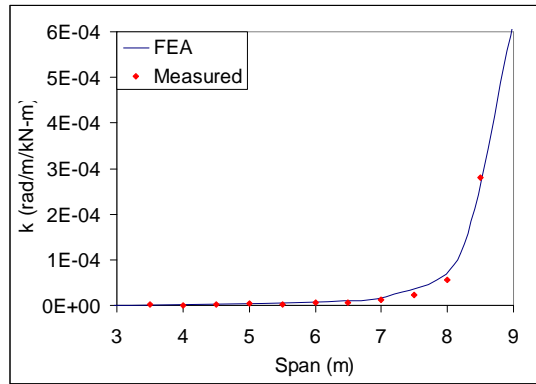


Figure 29. Twist Distribution of TX-100 – Measured and Predicted

2) Summary of Fatigue Tests. The CX-100, TX-100 and BSDS blades were successfully tested to the 20-year equivalent fatigue test loads (Fig. 30). The CX-100 needed to complete only 6,000 cycles at its initial load level to demonstrate adequate fatigue resistance but survived past 1.6 million cycles. The TX-100 design was a less stiff design and needed to survive to 2.0 million cycles under the load step regime. The blade failed at over 4 million cycles. BSDS failed at over 5 million cycles well past the target fatigue equivalent load. While further validation of the blade designs will occur upon completion of ongoing flight testing, the laboratory tests provide a favorable result for hybrid glass/carbon designs. Also of importance was that while the fatigue calculations were based on fiber direction material properties, the off-direction material properties played a role in the eventual failure of both blades. This demonstrates the difficulty in incorporating innovative design features in a fatigue sensitive structure and the difficulty of performing accurate fatigue life predictions based on limited, coupon-sized material property data and simple models.



Figure 30. TX-100 Fatigue Test at NREL's NWTC Facility

B. Knight & Carver Swept Blade

A Sandia contract with Knight & Carver (K&C) was started in 2005 to design and demonstrate a research blade that incorporates geometric sweep. The feasibility of using geometric sweep to reduce fatigue loads has been established in previous work at Sandia [36,37]. Reduced fatigue loads will allow for a longer blade for the same fatigue spectrum; thus the rotor swept area grows and more energy is captured. A 27-m swept blade (termed the STAR blade) has been designed and several fabricated. Static and fatigue tests are completed, and three additional blades are being flown on a machine in Tehachapi, California [59]. Figure 31 shows a mold for the STAR blade and a picture of the blades installed on the test turbine. Flight testing has confirmed that for an increase of 10% in blade length with sweep, the annual energy capture can be increased by at least 5-8%.



Figure 31. Knight & Carver Swept Blade Mold and Flight Testing

SUMMARY

This paper provides an overview and update of recent research results performed for Sandia's Wind Energy Department. This work is focused on developing large rotors that are lighter, more reliable and produce more energy. Included are discussions of research materials, manufacturing, load control (both passive and active), structurally efficient airfoils, noise reduction, and sensors. Also, several prototype blades have been successfully tested (fatigue, static and flight) and include innovations such as sweep, off-axis materials, carbon spars, and very thick airfoils (flatbacks) for inboard structural enhancements. The K&C STAR blade demonstrated that sweep-twist is a viable option for growing the rotor and passively capturing more energy. Sandia and NREL will continue to provide research in a variety of areas for the DOE Wind and Hydropower program.

REFERENCES

1. BTM Consult ApS, *World Market Update 2007*, Ringkobing, Denmark, March 2008.
2. U.S. DOE Energy Efficiency and Renewable Energy, "Wind Energy Multiyear Program Plan For 2007-2012," (www.energy.eere.gov).
3. U.S. DOE Energy Efficiency and Renewable Energy, "20% Wind Energy by 2030: Increasing Wind Energy's Contribution to U.S. Electricity Supply," (www.energy.eere.gov).
4. Ashwill, T., and Laird, D., "Concepts to Facilitate Very Large Blades," AIAA-2007-817, *Proceedings, ASME/AIAA Wind Energy Symposium*, Reno, NV, 2007.
5. Ashwill, T.D., "Developments in Large Blades for Lower Cost Wind Turbines", *Proceeding, AWEA 2004*, Chicago, Illinois.
6. TPI Composites, "Innovative Design Approaches for Large Wind Turbine Blades; Final Report," SAND2004-0074, Sandia National Laboratories, Albuquerque, NM.
7. Laird, D.L. and Ashwill, T.D., "Introduction to NuMAD: A Numerical Manufacturing and Design Tool," AIAA-98-0060, *Proceedings, ASME/AIAA Wind Energy Symposium*, Reno, NV, January 1998.
8. Lobitz, D.W. and Ashwill, T.D., "Aeroelastic Effects in the Structural Dynamic Analysis of Vertical Axis Wind Turbines," SAND85-0957, Sandia National Laboratories, Albuquerque, NM, 1986.
9. Lobitz, D.W., "Flutter Speed Predictions for MW-Sized Wind Turbine Blades," *Wind Energy Vol. 7, No.3*, 211-224, 2004.
10. Lobitz, D.W. and Veers, P.S., "Load Mitigation with Bending/Twist-Coupled Blades on Rotors Using Modern Control Strategies," *Wind Energy 2003*, 105-117.
11. Lobitz, D.W., "A NASTRAN-Based Computer Program for Structural Dynamic Analysis of Horizontal-Axis Wind Turbines," *Collected Papers on Wind Turbine Technology*, DOE/NASA/5776-2, NASA CR-195432, May 1995, 89-97.
12. Mandell, J.F. and Samborsky D.D., "DOE/MSU Composite Material Fatigue Database: Test Methods, Materials, and Analysis," SAND97-3002, Sandia National Laboratories, Albuquerque, NM, 1997.
13. Mandell, J.F. and Samborsky D.D., "DOE/MSU Fatigue of Composite Materials Database, 2008 Update." (www.sandia.gov/wind)
14. Mandell, J.F., Samborsky D.D. and Agastra, P., "Composite Materials Fatigue Issues in Wind Turbine Blade Construction," *SAMPE 2008*, Los Angeles, CA.

15. Samborsky D.D., Agastra, P. and Mandell, J.F., "Effects of Glass Fabric and Laminate Construction on the Fatigue of Resin Infused Blade Materials, *Proceedings, 2008 ASME/AIAA Wind Energy Symposium*, Reno, NV, 2008.
16. Griffin, D.A., "Blade System Design Studies Volume II: Final Project Report," SAND2009-0686, Sandia National Laboratories, Albuquerque, NM.
17. Mandell, J.F., Samborsky D.D., and Cairns, D.S., "Fatigue of Composite Materials and Substructures for Wind Turbine Blades," SAND2002-0771, Sandia National Laboratories, Albuquerque, NM, 2002.
18. Wilson, T.J., "Modeling of In-Plane and Interlaminar Fatigue Behavior of Glass and Carbon Fiber Composite Materials," *MS Thesis*, Department of Mechanical Engineering, Montana State University, 2006.
19. Mandell, J.F., Samborsky, D. D, and Wang, L., *SAMPE International Symposium*, 48, 2653, 2003.
20. Samborsky, D. D., Wilson, T. J. and Mandell, J. F., "Comparison of Tensile Fatigue Resistance and Constant Life Diagrams for Several Potential Wind Turbine Blade Laminates," *AIAA-2007-820, Proceedings, 2007 ASME Wind Energy Symposium*, Reno, NV, 2007.
21. Samborsky, D. D, Avery, D.P., Agastra, P., and Mandell, J.F., "Delamination and Failure at Ply Drops in Carbon Fiber Laminates Under Static and Fatigue Loading," *AIAA-2006-1195, Proceedings, 2006 ASME Wind Energy Symposium*, Reno, NV, 2006.
22. Griffin, D.A., "Blade System Design Studies Volume I: Composite Technologies for Large Wind Turbine Blades," SAND2002-1879, Albuquerque, NM, Sandia National Laboratories, July, 2002.
23. Griffin, D.A, "Blade System Design Studies Volume II: Preliminary Blade Designs and Recommended Test Matrix," SAND2004-0073. Albuquerque, NM, Sandia National Laboratories, June, 2004.
24. Cairns, D.S. and Skramstad, J.D., "Evaluation of Hand Lay-up and Resin Transfer Modeling in Composite Wind Turbine Blade Manufacturing," SAND2000-1425, Sandia National Laboratories, Albuquerque, NM, June 2000.
25. Mastbergen, D. B., "Simulation and Testing of Resin Infusion Manufacturing Processes for Large Composite Structures," SAND2006-7856P, Sandia National Laboratories, Albuquerque, NM, October 2007.
26. van Dam, C.P, Mayda, E., Chao, D., Jackson, K., Zuteck, M., and Berry, D., "Innovative Structural and Aerodynamic Design Approaches for Large Wind Turbine Blades," *AIAA-2005-0973, Proceedings, ASME/AIAA Wind Energy Symposium*, Reno, NV, 2005.
27. Standish, K.J. and van Dam, C.P., "Aerodynamic Analysis of Blunt Trailing Edge Airfoils," *J.Solar Energy Engineering*, 125:479-487, 2003.
28. Barone, M.F. and Berg, D., "Aerodynamic and Aeroacoustic Properties of a Flatback Airfoil: An Update," *AIAA-2009-271, 47th AIAA Aerospace Sciences Meeting and Aerospace Exposition*, Orlando, Florida, 2009.
29. Baker, J.P., Mayda, E.A., and van Dam, C.P., "Experimental and Computational Analysis of Thick Flatback Wind Turbine Airfoils," *AIAA-2006-193, Proceedings, ASME/AIAA Wind Energy Symposium* Reno, Nevada, 2006.
30. Chao, D.D and van Dam, C.P., "Computational Aerodynamics Analysis of a Blunt Trailing-Edge Airfoil Modification to the NREL Phase VI Rotor, *Wind Energy*, 10(6):529-550, 2007.
31. P. S. Veers, G. Bir and D. W. Lobitz, "Aeroelastic Tailoring in Wind-Turbine Blade Applications," *Proceedings, Windpower '98 Meeting*, pp. 291-304.
32. Lobitz, D. and Veers, P., "Aeroelastic Behavior of Twist-coupled HAWT Blades," *Proceedings, ASME/AIAA Wind Energy Symposium*, Reno, NV, 1998, pp. 75-83.
33. Lobitz, D. and Laino, D., "Load Mitigation with Twist-coupled HAWT Blades," *Proceedings, ASME/AIAA Wind Energy Symposium*, Reno, NV, 1999, pp. 124-134.
34. D. Lobitz, P. S. Veers and D. J. Laino, "Performance of Twist-Coupled Blades on Variable Speed Rotors," *Proceedings, ASME/AIAA Wind Energy Symposium*, Reno, NV, 2000, pp. 404-412.
35. D. W. Lobitz et al., "The Use of Twist-Coupled Blades to Enhance the Performance of Horizontal Axis Wind Turbines," SAND2001-1303, Albuquerque, NM, May 2001.
36. Ashwill, T.D., Veers, P.S., Griffin, D., Locke, J., Contreras, I., Zuteck, M.D., "Concepts for Adaptive Wind Turbine Blades," *AIAA-2002-28, Proceeding, ASME/AIAA Wind Energy Symposium*, Reno, NV, 2002.
37. Zuteck, M.D., "Adaptive Blade Concept Assessment: Curved Planform Induced Twist Investigation," SAND02-2996, Albuquerque, NM, 2002.
38. Ong, C.H., Wang, J., and Tsai, S.W., "Design, Manufacture and Testing of a Bend-Twist D-Spar," *AIAA-1999-25, Proceeding, ASME/AIAA Wind Energy Symposium*, Reno, NV, 1999.
39. Stol, K. A.; Zhao, W.; Wright, A. D. (2006). "Individual Blade Pitch Control for the Controls Advanced Research Turbine (CART)". *Journal of Solar Energy Engineering, Transactions of the ASME*. Vol. 128(4), November 2006; pp. 498-505; NREL Report No. JA-500-41019.
40. Johnson, S.J., van Dam, C.P., and Berg, D.E., "Active Load Control Techniques for Wind Turbines," SAND2008-4809, Sandia National Laboratories, Albuquerque, NM, August 2008.
41. Yen-Nakafuji, D.T., van Dam, C.P., Smith, R.L., and Collings, S.D., "Active Load Control for Airfoils Using Microtabs," *Journal of Solar Energy Engineering*, Vol. 123, No. 4, Nov. 2001, pp. 282-289.

42. Yen, D.T., van Dam, C.P., Brauchle, F., Smith, R.L., and Collings, S.D., "Active Load Control and Lift Enhancement Using MEM Translational Tabs," AIAA-2000-2422, *Fluids 2000*, Denver, CO, June 2000.
43. Baker, J.P., Standish, K.J., and van Dam, C.P., "Two-Dimensional Wind Tunnel and Computational Investigation of a Microtab Modified S809 Airfoil," AIAA 2005-1186, *43rd AIAA Aerospace Sciences Meeting and Exhibit*, Reno, NV, 2005.
44. Wilson, D.G., Berg, D.E., Lobitz, D.W., and Zayas, J.R., "Optimized Active Aerodynamic Blade Control for Load Alleviation on Large Wind Turbines," *AWEA WINDPOWER 2008 Conference & Exhibition*, June 2008.
45. Barlas, T.K., and van Kuik, G.A.M., "State of the Art and Prospectives of Smart Rotor Control for Wind Turbines", *The Science of Making Torque from Wind, Journal of Physics: Conference Series 75 (2007) 012080*.
46. Bak, C., Gaunna, M., Anderson, P., Buhl, T., Hansen, P., Clemensen, K., and Moeller, R., "Wind Tunnel Test on Wind Turbine Airfoil with Adaptive Trailing Edge Geometry", *45th AIAA Aerospace Sciences Meeting and Exhibit*, Reno, Nevada, 8-11 January, 2007.
47. Lackner, Matthew and van Kuik, Gijs, "A Comparison of Smart Rotor Control Approaches using Trailing Edge Flaps and Individual Pitch Control", *47th AIAA Aerospace Sciences Meeting and Exhibit*, Orlando, Florida, 5-8 January, 2009.
48. Zayas, J.R., van Dam, C.P., Chow, R., Baker, J.P., and Mayda, E.A., "Active Aerodynamic Load Control for Wind Turbine Blades", *European Wind Energy Conference*, Milan, Italy, 7-10 May, 2007.
49. Kota, Sridhar, Hetrick, Joel A., Osborn, Russell, Paul, Donald, Pendleton, Edmund, Flick, Peter, and Tilmann, Carl, "Design and Application of Compliant Mechanisms for Morphing Aircraft Structures", *Proc. SPIE 5054*, 24 (2003), DOI:10.1117/12.483869.
50. Berg, D.E., Wilson, D.G., Barone, M.F., Resor, B.R., Berg, J.C., Paquette, J.A., Zayas, J.R., Kota, S., Ervin, G. and Maric, D., "The Impact of Active Aerodynamic Load Control on Fatigue and Energy Capture at Low Wind Speed Sites" *EWEC 2009*, March 2009.
51. Cairns, D.S., Palmer, N., and Ehresman, J., "Low Cost Inspection for Improved Blade Reliability," AIAA 2009-1408, *47th AIAA Aerospace Sciences Meeting and Exhibit*, Orlando, Florida, 5-8 January, 2009.
52. White, J.R., Adams, D.E., and Rumsey, M.A., "Operational Load Estimation of a Smart Wind Turbine Rotor Blade," *2008 SPIE Smart Structures and Materials & Nondestructive Evaluation and Health Monitoring*, San Diego, California, March 2008.
53. Rumsey, M.A. and Paquette, J.A., "Structural Health Monitoring of Wind Turbine Blades", *2008 SPIE Smart Structures and Materials & Nondestructive Evaluation and Health Monitoring*, San Diego, California, March 2008.
54. Griffin, D. A., "Blade System Design Studies Volume II: Preliminary Blade Designs and Recommended Test Matrix," SAND2004-0073, Sandia National Laboratories, Albuquerque, NM, June 2004.
55. TPI Composites, Inc., "Blade Manufacturing Improvements Development of the ERS-100 Blade," SAND2001-1381, May 2001.
56. Ashwill, T.D. and Paquette, J.P., "Composite Materials for Innovative Wind Turbine Blades," *SAMPE 2008*, Los Angeles, CA, May 2008.
57. Berry, D., "Design of 9-Meter Carbon-Fiberglass Prototype Blades: CX-100 and TX-100," SAND2007-0201, Sandia National Laboratories, Albuquerque, NM, September 2007.
58. Paquette, J.P. and Veers, P.S., "Increased Rotor Size through Passive Load Control and Weight Reduction Concepts," *EWEC 2009*, March 2009.
59. Ashwill, T.D. and Kanaby, G., "Sweep-Twist Adaptive Blade," *EWEC 2007*, May 2007.